1

2

TITLE

4 Targeting T-cell receptor β-constant for immunotherapy of T-cell malignancies

5

6

AUTHORS

8 Paul M. Maciocia[1], Patrycja A. Wawrzyniecka[1], Brian Philip[1], Ida Ricciardelli[2], Ayse U.

9 Akarca[1], Shimobi Onuoha[3], Mateusz Legut[4], David K. Cole[4], Andrew K. Sewell[4],

10 Giuseppe Gritti[5], Joan Somja[6], Miguel A. Piris[7], Karl S. Peggs[1], David C. Linch[1], Teresa

11 Marafioti[1], Martin A. Pule[1,3]*

12

13 [1] University College London, Cancer Institute, London, UK

14 [2] University College London, Institute of Child Health, London, UK

15 [3] Autolus Ltd, London, UK

16 [4] Division of Infection and Immunity, Cardiff University School of Medicine, UK

17 [5] Department of Haematology, Papa Giovanni XXII Hospital, Milan, Italy

18 [6] Department of Anatomy and Cellular Pathology, University of Liege, Belgium

19 [7] Anatomical Pathology Service, University Hospital Marques de Valdecilla (IFIMAV),

20 Santander, Spain

21

22 * Corresponding author

23

32

33

34

35

CONTRIBUTIONS

37   PM designed and performed the experimental work and wrote the manuscript. PW

38   performed experimental work. BP designed and performed *in vivo* experiments, and

39   wrote the manuscript. IR generated and tested EBV-CTLs. AA performed

40   immunohistochemistry. SO, DC and AS produced soluble TCR molecules, performed

41   surface plasmon resonance analysis and wrote the manuscript. ML and AK identified

42   and characterised iNKTs. GG, JS and M.Piris supplied clinical samples. KP and DL

43   helped design experiments and wrote the manuscript. TM optimised and analysed

44   immunohistochemical staining, and wrote the manuscript. M.Pule conceived the idea,

45   designed the experimental work and wrote the manuscript.

46

47

48

49   **ABSTRACT**

50

51   Mature T-cell cancers are typically aggressive, treatment-resistant and associated with

52   poor prognosis. Translation of immunotherapeutic approaches has been limited by a

53   lack of target antigens discriminating malignant from healthy T-cells. Unlike B-cell

54   depletion, pan T-cell aplasia is prohibitively toxic. We report a novel targeting strategy

55   based on the mutually exclusive expression of either *TRBC1* or *TRBC2* T-cell receptor

56   (TCR) β-constant domain. We identify an antibody with unique TRBC1 specificity, and

57   use this to rapidly screen for T-cell clonality, demonstrating that while normal and viral-

58   specific T-cells contain TRBC1 and TRBC2 compartments, malignancies are restricted

59   to only one. As proof of concept for anti-TRBC immunotherapy, we developed anti-

60   TRBC1 CART-cells, which recognise and kill normal and malignant TRBC1 but not

61   TRBC2 T-cells, *in vitro* and in a disseminated murine leukaemia model. Unlike non-

62   selective approaches targeting the entire T-cell population, TRBC-targeted

63   immunotherapy could eradicate a T-cell malignancy while preserving sufficient normal

64   T-cells to maintain cellular immunity.

65

66

67

68

69   **INTRODUCTION**

70

71   Mature T-cell lymphomas (PTCLs) are a heterogeneous group of disorders,

72   collectively comprising 10-15% of non-Hodgkin's lymphoma[1]. These cancers typically

73   behave aggressively[2,3]. Outcomes are worse than equivalent B-cell cancers, with an

74   overall estimated 5-year survival of only 32%[3]. Furthermore, while treatment of B-cell

75   cancers benefits from targeted immunotherapies such as therapeutic monoclonal

76   antibodies (mAbs)[4], bispecific T-cell engagers[5] and more recently chimeric antigen

77   receptor (CAR) T-cell therapy[6,7], no such approaches are available for T-cell cancers.

78

79   Immunotherapies used in B-cell malignancies target pan B-cell antigens, since no

80   antigens exist which discriminate normal from malignant B-cells. The consequent

81   depletion of the normal B-cell compartment is surprisingly well tolerated and is

82   considered an acceptable side-effect[6,7]. The situation is different with T-cells: once

83   again, no antigens exist which discriminate normal from malignant T-cells[3,8]; however,

84   T-cell aplasia consequent to targeting a pan T-cell antigen would lead to profound and

85   unacceptable immunosuppression[9]. Here, we describe a targeting approach for

86   treating mature T-cell cancers which relies on recognition of a pan T-cell antigen, but

87   avoid severe immunosuppression.

88

89   The α/β T-cell receptor (TCR) is a pan T-cell antigen. Apart from its expression on

90   normal T-cells it is an ideal target: it is expressed by >95% of cases of PTCL-NOS[8],

91   almost all AITL[8], as well as 30% of T-acute lymphoblastic leukaemia (T-ALL)[10]. High

92   and homogenous surface expression is commonly seen on lymphoma cells[11] and in

93   addition, evidence exists that a proportion of PTCL cases may depend on TCR-

94   associated signalling for lymphomagenesis and survival[12]. TCR α and β chains

95   comprise amino-terminal variable and carboxy-terminal constant regions[13] (Figure 1a).

96   TCR diversity is generated by somatic recombination, when each TCR chain selects a

97   variable (V), diversity (D), joining (J) and constant (C) region[13]. Importantly, cells of a

98   clonal T-cell population all express the same unique TCR. However, approaches

99   targeting TCR variable regions unique to a malignant clone are impracticable, since a

100   bespoke therapeutic is required for each patient.

101

102   An oft-forgotten feature of TCR β-chain recombination is that there are two β-constant

103   region genes: TRBC1 and TRBC2. Each TCR (and therefore each T-cell) expresses,

104   mutually exclusively and irreversibly, TCR β-constant coded by either TRBC1 or

105   TRBC2[14,15] (Figure 1b). Hence, normal T-cells will be a mixture of individual cells

106   expressing either TRBC1 or 2, while a T-cell cancer will express either TRBC1 or 2 in

107   its entirety. We propose targeting TRBC1 in case of a TRBC1+ T-cell malignancy, or

108   the converse in case of a TRBC2+ malignancy. This will target all cells of the malignant

109   clone, but leave a substantial proportion of the T-cell compartment intact.

110

111   In this work, we demonstrate that it is possible to distinguish between TRBC1 and 2

112   TCRs with an antibody, despite almost identical amino acid sequences (Figure 1c).

113   We show that peripheral blood T-cells in normal subjects comprise of a mixture of

114   approximately 35:65% TRBC1/2 cells, and that complete depletion of either TRBC1 or

115   2 compartments will still maintain adequate viral immunity. We confirm TRBC clonality

116   in   many   types   of   T-cell   malignancies   by   both   flow   cytometry   and

117   immunohistochemistry. Finally, we demonstrate efficacy of a CAR with TRBC1

118   specificity to prove our targeting concept.

119

120

121   **RESULTS**

122

123   **JOVI-1 mAb is specific for TRBC1-expressing cells**

124

125   To find a TRBC specific binder, we screened anti-TCR mAbs which are known to bind

126   a proportion of T-cells in peripheral blood. In order to screen for TRBC1/2 specificity

127   we cloned the α and β-chains of the well-characterised HA-1 TCR[16] in TRBC2 (native)

128   format or with mutations introduced in the constant domain to convert to TRBC1. We

129   stably expressed either TCR on the surface of Jurkat T-cell line with knocked out TCR

130   α and β loci (JKO). Analysis by flow cytometry demonstrated that, while both TRBC1-

131   JKO and TRBC2-JKO lines expressed surface TCR/CD3, mAb JOVI-1[17] recognised

132   only TRBC1-JKO cells and not TRBC2-JKO cells (Figure 1d), confirming the TRBC1

133   specificity of this antibody. Surface plasmon resonance analysis demonstrated that

134   JOVI-1 bound to a TRBC1-TCR with an affinity of K_D = 0.42nM and a half-life of

135   ~30mins, in line with other therapeutic antibodies[18]. In contrast, JOVI-1 binding to a

136   TRBC2-TCR was >10,000x weaker, demonstrating the remarkable specificity of the

137   reagent (supplementary Figure 1).

138

139   TCR β-junctional regions segregate with constant domains: TCRs selecting TRBJ1 1-

140   6 use TRBC1, and those selecting TRBJ2 1-7 use TRBC2[13]. It was therefore possible

141   that JOVI-1 only maintains TRBC1-specificity in the context of particular junctional

142   regions. We cloned several TCRs of varying antigen specificity, utilising a range of

143   variable/ junctional regions, from publicly available sequences. When transfected into

144   human embryonic kidney (HEK)-293T cells along with a plasmid supplying the

145   components of CD3, TCRs were expressed on the cell surface. JOVI-1 uniformly

146   recognised TRBC1 cells despite varying TRBJ1 regions, and did not recognise cells

147   expressing TRBC2 TCRs and varying TRBJ2 regions (Figure 1e). In addition, we

148   cloned a truncated TCR lacking α and β V(D)J domains. CD3 staining confirmed

149   surface assembly, and staining with JOVI-1 was similar to that seen with full-length

150   TCR (Figure 1f). This offered further confirmation that junctional regions were not

151   required for the JOVI-1 epitope.

152

153   We then sought to determine the residues of TRBC responsible for the TRBC1-

154   specificity of JOVI-1. Structural analysis suggested that the F->Y at residue 36 is

155   buried in secondary structure and V->E at residue 135 is likely too close to the

156   membrane to be accessible. However, the NK->KN difference at residues 4-5 is

157   exposed to the surface and represents a substantial difference of both shape and

158   charge to the epitope. By introducing each mutation required to convert TRBC2 to

159   TRBC1 individually, we confirmed that the reversal of asparagine and lysine residues

160   at positions 3-4 was indeed the discriminating portion of the JOVI-1 epitope (Figure

161   1f,g).

162

163

164   **Normal αβ T-cells contain a mixture of TRBC1+ and TRBC1- populations**

165

166   Using JOVI-1, we then sought to determine the proportion of T-cells from normal

167   donors that were TRBC1 versus TRBC2. Each donor had TCR+TRBC1+ and

168   TCR+TRBC1- cells in both CD4 and CD8 compartments, with median TRBC1

169   expression of 35% (range 25-47%, Figure 2a,b). We also confirmed that CD4 and CD8

170   differentiation subsets all contained both populations with a similar TRBC1:TRBC2

171   ratio (Suppl Fig 2a,d). In addition, we identified 2 cell types which express a semi-

172   invariant restricted TCR repertoire, mucosal-associated invariant T-cells (MAITs, suppl

173   Fig 2b,d) and invariant natural killer/ T-cells (iNKTs, suppl Fig 2c,d) and demonstrated

174   that these populations also contain both TRBC1+ and TRBC1- cells, albeit with a lower

175   TRBC1 proportion than seen in bulk T-cell populations.

176

177

178   Although the polyclonal T-cell population in normal donors contained both TRBC1 and

179   TRBC2 cells, we reasoned that the T-cell response to a particular virus may be skewed

180   towards one of these, and therefore that removal of one subset could result in loss of

181   cellular immunity. To determine if this was the case, we generated oligoclonal Epstein

182   Barr Virus (EBV)-specific cytotoxic T-cell lines from normal donors, as previously

183   described[19]. These cells lysed autologous EBV-transformed cells (Figure 2c). Staining

184   in 3 donors revealed the cells were >98% CD8+ (data not shown) and contained a

185   mixed population of TRBC1+ and TRBC1- (median 45% TRBC1+) cells,

186   demonstrating that the T-cell response to EBV contains both populations (Figure 2d).

187   In addition, we identified T-cells specific for cytomegalovirus (CMV) or adenovirus

188   (AdV) by incubation of peripheral blood mononuclear cells (PBMCs) with pools of

189   antigenic peptides. Viral-specific T-cells, identified by interferon-gamma (IFN-γ)

190   expression after peptide incubation (Figure 2e), were found to contain both TRBC1+

191   and TRBC1- cells (Figure 2f). Summary data from normal donors demonstrated

192   median TRBC1 expression of 45% (CMV) and 41% (AdV) (Figure 2g).

193

194

195   **T-cell derived malignant cell lines and primary T-cell tumours are clonally**
196   **TRBC1+ or TRBC1-**

197

198   Surface TCR+ cell lines were stained with JOVI-1 and were found to be either TRBC1+
199   (H9, Jurkat, MJ) or TRBC1- (HD-Mar2, HPB-ALL, T-ALL1, HH, T-ALL1). TRBC1
200   versus TRBC2 expression was confirmed at the transcriptional level by PCR
201   amplification of the β-constant region from cDNA, followed by Sanger sequencing
202   (Figure 3a). These data confirmed JOVI-1 as a marker of TRBC1 clonality in cell lines.
203   Next, using multiparameter flow cytometry, we analysed primary blood samples from
204   several patients with T-large granular leukaemia (T-LGL), a TCR+ lymphoproliferative
205   disorder characterised by circulating tumour cells which express CD57[20]. While
206   CD57+ tumour cells demonstrated markedly skewed TRBC1:TRBC2 ratios, normal
207   CD4+ and CD8+ T-cells displayed appropriate ratios of each population (Figure 3b).
208   Using intracellular staining, we replicated this finding in primary marrow samples of T-
209   ALL (Figure 3c). Further, using flow cytometry (FACS) or immunohistochemistry (IHC)
210   on frozen tissue sections, we stained a number of primary samples of TCR+
211   malignancies of multiple histologies and confirmed that TRBC1 staining could be used
212   to determine if tumours were clonally TRBC1+ or TRBC1- (Figure 3d,e). In 58 samples
213   (38 analysed by IHC, 20 by FACS), 40% were TRBC1+ and 60% were TRBC1- (Figure
214   3f). Of note, TCR/CD3 expression assayed by FACS in primary tumours was typically
215   at a similar level to admixed normal T-cells (median MFI = 96% of normal T-cell MFI),
216   other than in adult T-cell leukaemia/ lymphoma (ATLL) where expression was typically
217   dimmer than in normal T-cells (median MFI 23% of normal T-cell MFI, Fig 3g).

218

219   **T-cells transduced with anti-TRBC1 CAR specifically target TRBC1+ but not**
220   **TRBC2+ cells *in vitro***

221

222   As a proof of concept for therapies targeting TRBC we cloned a single-chain variable
223   fragment based on the JOVI-1 antibody into a 3rd generation CAR format[21]. We
224   retrovirally transduced T-cells from normal donors to stably express this construct, and
225   confirmed surface expression of CAR on up to 90% of cells (Fig 4a). We subsequently
226   co-cultured non-transduced (NT) or anti-TRBC1 CAR T-cells with NT-JKO, TRBC1-
227   JKO or TRBC2-JKO cells. While NT effectors did not secrete IFN-γ in response to any
228   target cells, TRBC1 CAR T-cells specifically released IFN-γ only when incubated with
229   TRBC1-JKO and not NT-JKO or TRBC2-JKO cells (Figure 4b,c). In 4hr chromium
230   release cytotoxicity assays, NT cells did not display cytotoxicity, while anti-TRBC1

231 CAR T-cells specifically killed TRBC1-JKO and not NT-JKO or TRBC2-JKO cells

232 (Figure 4d,e).

233

234 In addition, we performed flow cytometric cytotoxicity assays using multiple α/ β TCR+

235 cell lines as targets, and confirmed killing of TRBC1+ but not TRBC2+ cell lines by

236 anti-TRBC1 CAR T-cells, while NT T-cells did not lyse either (Figure 4f). Next, to

237 simulate a physiological setting, we mixed TRBC1-JKO cells labelled with CD19

238 marker gene at 1:1 ratio with TRBC2-JKO cells labelled with blue fluorescent protein

239 (BFP). This population was co-cultured with anti-TRBC1 CAR-T or NT cells. Analysis

240 at 48hrs confirmed eradication of TRBC1 cells with preservation of TRBC2 cells by

241 anti-TRBC1 CAR, and no killing of either population seen with NT effectors (Figure

242 4g).

243

244 We obtained primary tumour cells from multiple patients with TRBC1+ T-cell

245 malignancies. We co-cultured patient tumour with NT or anti-TRBC1 CART-cells at a

246 1:1 ratio. Using allogeneic T-cells, we demonstrated specific kill of tumour in cases of

247 T-prolymphocytic leukaemia (T-PLL) and PTCL-NOS, with preservation of a

248 substantial proportion of residual normal T-cells (Figure 4h). Tumour kill was seen

249 even in cases of ATLL (Figure 4i,l), where TCR/CD3 was partially downregulated from

250 the cell surface (Figure 2g). In addition, we demonstrated successful transduction of

251 T-cells from a patient with TRBC1+ malignancy (ATLL) despite heavy circulating

252 tumour burden (Figure 4j), that the T-cell product was 'purged' of contaminating tumour

253 cells (Figure 4k) and that anti-TRBC1 CAR specifically killed autologous tumour cells

254 (Figure 4l).

255

256 **Anti-TRBC1 CAR-T cells selectively deplete normal TRBC1, but not TRBC2 cells**

257

258 Following anti-TRBC1 CAR transduction, no TRBC1+ cells could be detected in either

259 the transduced or non-transduced fractions, indicating possible depletion of this

260 population (Suppl Fig 3a). However, we reasoned that absent TRBC1 staining was

261 likely due to epitope blocking by ligated anti-TRBC1 CAR. Therefore, we transduced

262 cells with anti-TRBC1 CAR and CD34 marker gene[22]. This enabled sorting of cells into

263 CAR+ and CAR- fractions using CD34-bead magnetic depletion. We confirmed

264 depletion of all CAR+ cells in the –ve fraction, thus excluding any effect of epitope

265 blockade by CAR. While NT cells contained both TRBC1+ and TRBC1- fractions, the

266 CAR –ve fraction did not contain any TRBC1+ cells, confirming selective depletion of

267 TRBC1 cells (Suppl Figure 3b). Further, we sorted normal donor T-cells into TRBC1+

268   and TRBC1- populations using magnetic beads. We subsequently separately labelled

269   each population with different fluorescent nuclear dyes, enabling later discrimination

270   of the populations, and co-cultured with autologous NT or anti-TRBC1 CART-cells.

271   While TRBC2 cells co-cultured with anti-TRBC1 CAR were not depleted compared to

272   NT condition, TRBC1 cells were 80% depleted at 7 days (Suppl Figure 3c), indicating

273   selective purging of this population. This was confirmed in a further assay, in which

274   TRBC1 cells were mixed at a 1:2 (physiological) ratio with TRBC2 cells before 1:1 co-

275   culture with NT or anti-TRBC1 cells. At 7 days, virtually all TRBC1 cells had been

276   depleted from the culture, while TRBC2 cells remained (Suppl Fig 3d). Finally, to

277   further mitigate against potential transduction of contaminating TRBC1 tumour cells,

278   we pre-depleted normal donor T-cells of TRBC1+ cells to obtain cells which were >99%

279   TRBC1- (Supplementary Figure 3e), then demonstrated transduction with anti-TRBC1

280   CAR that was similar to that achieved for unsorted cells (Supplementary Figure 3f).

281

282

283   **Anti-TRBC1 CAR-T cells specifically killed TRBC1+ tumour while preserving**

284   **TRBC2+ tumour in murine models of disseminated T-cell malignancy.**

285

286   We utilised an established murine xenograft model of disseminated T-cell leukaemia.

287   Non-obese diabetic-severe combined immunodeficiency γ-chain–deficient (NSG) mice

288   (Jackson) were intravenously injected with Jurkat T-cells, which natively express a

289   TRBC1 TCR at a level similar to primary tumour and normal T-cells (Figure 2g). Jurkat

290   cells were modified to stably express firefly luciferase (F-Luc) and CD19 marker gene,

291   and stably engrafted in the bone marrow of all injected animals by day 6 (Figure 5a,b).

292   Following engraftment, we treated mice with T-cells expressing anti-TRBC1 CAR or a

293   control (irrelevant) CAR. Mice treated with anti-TRBC1 CAR had dramatic tumour

294   reduction by BLI at D10 (Figure 5b,c), and this was associated with a substantial

295   survival benefit. In a further experiment to evaluate CAR persistence (Figure 5e), we

296   demonstrated tumour clearance and increased numbers of anti-TRBC1 versus control

297   CAR T-cells in peripheral blood at D21 following T-cell injection (Figure 5f). Bone

298   marrow was harvested at the time of death (survivors culled at D42), with similar results

299   seen (Figure 5g).

300

301   Next, we injected a further cohort of mice with equal proportions of Jurkat-TRBC1 cells

302   (human CD19 marker gene) and JKO cells engineered to express TRBC2 TCR and

303   BFP marker gene). Tumour engraftment in marrow was confirmed in all animals by BLI

304   at day 6. Animals were then treated with NT or anti-TRBC1 CAR T-cells. Flow

305   cytometry of bone marrow confirmed the TRBC1 specificity of anti-TRBC1 CAR T-cells

306   *in vivo*: while mice receiving NT effectors had approximately equal proportions of

307   Jurkat-TRBC1 and JKO-TRBC2 cells in marrow, only JKO-TRBC2 cells were seen in

308   recipients of anti-TRBC1 CAR T-cells (Figure 5e,f).

309

310   Finally, in order to determine if anti-TRBC1 CAR was able to deplete TRBC1 tumour

311   in a physiological setting (ie in the presence of normal T-cells), we engrafted NSG mice

312   with Jurkat-CD19-Fluc tumour as before. After 7 days, mice were injected with human

313   PBMCs (Supplementary Fig 4a). After a further 7 days, human monocyte and T-cell

314   engraftment was confirmed by flow cytometry of peripheral blood (Supplementary Fig

315   4b), and progressive disease was demonstrated by BLI (Supplementary Fig 4c).

316   Animals were then injected with anti-TRBC1 CAR or control CAR, with cells prepared

317   from the same donor as initial PBMCs. BLI and flow cytometry of bone marrow at 5

318   days following treatment demonstrated tumour control in anti-TRBC1 CAR recipients,

319   but disease progression in control CAR recipients (Supplementary Fig 4c,d,e). Flow

320   cytometry of bone marrow (Supplementary Figure 4e) and spleen (Supplementary

321   Figure 4f) at D6 demonstrated similar numbers of non-CAR T-cells were present in

322   anti-TRBC1 and control CAR recipients, confirming persistence of normal T-cells in

323   the face of tumour depletion.

324

325

326

327

11

328 **DISCUSSION**

329

330 The presence of two functionally identical genes at the TCR-β constant region has

331 been recognised for more than 30 years[14,15], but has not been exploited until now. We

332 have demonstrated that despite highly similar amino acid sequences, it is possible to

333 discriminate between TRBC1 and TRBC2 proteins on normal and malignant T-cells.

334 Indeed, JOVI-1 demonstrated >10,000-fold difference in binding affinity, with specificity

335 based on the reversal of only 2 residues in TRBC. Consistent with previous findings,

336 we have shown that approximately 2/3 of both normal T-cells[23,24] and T-cell cancers[25]

337 express TRBC2-TCR.

338

339 We believe TRBC1/2 targeting has considerable potential for immunotherapy of T-cell

340 malignancies. The principle of using immunotherapy to target a rearranged clone-

341 specific receptor is not new: Stevenson *et al* pioneered the use of patient-specific anti-

342 idiotype mAbs against neoplastic lymphoma cells[26,27]. However, this approach is

343 impracticable since it requires a novel binder to be generated for each patient. An

344 analogous approach to ours, targeting B-cell cancers with antibody light-chain specific

345 therapy has also been proposed[28].

346

347 Patients with B-cell malignancies have greatly benefited from the advent of potent

348 immunotherapies. Rituximab, usually given in combination with cytotoxic

349 chemotherapy, has dramatically improved outcomes in indolent[29] and aggressive B-

350 cell lymphomas[30] and is now part of standard front-line therapy. Further agents

351 including depleting antibodies, radio-immune conjugates, bi-specific T-cell engagers

352 and other modalities have also proven effective and are in widespread use[31]. Of

353 immunotherapies in development, perhaps the most promising approach is CAR T-

354 cells. Treatment of B-cell malignancies with anti-CD19 CART-cells has been one of

355 the most important recent advances in the treatment of cancer, with sustained

356 remissions obtained in most patients with advanced and refractory B-ALL[6,32], as well

357 as impressive though lesser responses in CLL[7,33] and diffuse large B-cell lymphoma[7].

358 Given the relatively similar presentation and nature of B- and T-cell malignancies,

359 CART-cells could potentially have similar value in treating T-cell lymphomas.

360

361 However, anti-CD19 CART efficacy is accompanied by loss of the normal B-cell

362 compartment[6,7]. While this is relatively well tolerated, and impact can be lessened by

363 infusion of donor–derived pooled immunoglobulins, analogously targeting a pan-T-cell

364   antigen on a T-cell malignancy (with concomitant permanent loss of normal T-cells)

365   would be prohibitively toxic, with no mitigating replacement therapies available.

366

367   Approaches using CARs against T-cell targets such as the pan T-cell antigen CD5[34]

368   or CD4, which is present on a crucial subset of normal T-cells[35], have been proposed,

369   but may prove unacceptably immunosuppressive in clinical use. With our approach, a

370   patient treated with anti-TRBC1 CART would retain approximately 2/3 of normal T-

371   cells, with polyclonal anti-viral immunity likely preserved. In addition, the potential for

372   'on-target off-tumour' toxicity affecting other tissues would be negligible, given the

373   restriction of TCR expression to mature T- or NK/T-cells. However, with any approach

374   targeting T-cells rather than B-cells increased cytokine-mediated toxicity could occur,

375   due to lysis of normal tissue-resident T-cells and subsequent mediator release.

376   Another potential consequence of depletion of part of the regulatory T-cell repertoire

377   could be loss of some peripheral tolerance, if the T-regulatory cells protecting a

378   particular tissue were particularly skewed towards TRBC1 or 2. However, ultimately

379   the toxicities associated with depletion of TRBC1 or 2 cells could only be examined in

380   a clinical trial.

381

382   In summary, we have demonstrated a novel approach to investigation and targeting of

383   T-cell malignancies by distinguishing between two possible TCR beta-chain constant

384   regions. Using CART-cells targeting one constant region we have demonstrated proof

385   of concept. Exploration of the distribution of constant region usage by unselected

386   normal T-cells and those providing specific viral immunity suggests that such an

387   approach would not lead to significant immunosuppression. We hope that this

388   approach heralds the application of potent targeted immunotherapeutics to provide

389   much needed enhancement of the treatment of T-cell malignancies.

390

391

392

393   **REFERENCES**

394

395   1.   A clinical evaluation of the International Lymphoma Study Group classification
396   of non-Hodgkin's lymphoma. The Non-Hodgkin's Lymphoma Classification
397   Project. *Blood* **89,** 3909–3918 (1997).
398   2.   Vose, J., Armitage, J., Weisenburger, D.International T-Cell Lymphoma
399   Project. International peripheral T-cell and natural killer/T-cell lymphoma study:
400   pathology findings and clinical outcomes. *Journal of Clinical Oncology* **26,**
401   4124–4130 (2008).
402   3.   Weisenburger, D. D. *et al.* Peripheral T-cell lymphoma, not otherwise
403   specified: a report of 340 cases from the International Peripheral T-cell
404   Lymphoma Project. *Blood* **117,** 3402–3408 (2011).
405   4.   Gao, G. *et al.* A systematic review and meta-analysis of immunochemotherapy
406   with rituximab for B-cell non-Hodgkin's lymphoma. *Acta Oncol* **49,** 3–12
407   (2010).
408   5.   Bargou, R. *et al.* Tumor regression in cancer patients by very low doses of a T
409   cell-engaging antibody. *Science* **321,** 974–977 (2008).
410   6.   Maude, S. L. *et al.* Chimeric Antigen Receptor T Cells for Sustained
411   Remissions in Leukemia. *N Engl J Med* **371,** 1507–1517 (2014).
412   7.   Kochenderfer, J. N. *et al.* Chemotherapy-refractory diffuse large B-cell
413   lymphoma and indolent B-cell malignancies can be effectively treated with
414   autologous T cells expressing an anti-CD19 chimeric antigen receptor. *Journal
415   of Clinical Oncology* **33,** 540–549 (2015).
416   8.   Went, P. *et al.* Marker expression in peripheral T-cell lymphoma: a proposed
417   clinical-pathologic prognostic score. *Journal of Clinical Oncology* **24,** 2472–
418   2479 (2006).
419   9.   Notarangelo, L. D., Kim, M.-S., Walter, J. E. & Lee, Y. N. Human RAG
420   mutations: biochemistry and clinical implications. *Sci Rep* 1–13 (2016).
421   doi:10.1038/nri.2016.28
422   10.   Pui, C. H. *et al.* Heterogeneity of presenting features and their relation to
423   treatment outcome in 120 children with T-cell acute lymphoblastic leukemia.
424   *Blood* **75,** 174–179 (1990).
425   11.   Jamal, S. *et al.* Immunophenotypic analysis of peripheral T-cell neoplasms. A
426   multiparameter flow cytometric approach. *Am. J. Clin. Pathol.* **116,** 512–526
427   (2001).
428   12.   Palomero, T. *et al.* Recurrent mutations in epigenetic regulators, RHOA and
429   FYN kinase in peripheral T cell lymphomas. *Sci Rep* **46,** 166–170 (2014).
430   13.   Delves, P. J., Martin, S. J. & Roitt, D. R. B. A. I. M. Roitt's Essential
431   Immunology. 1–562 (2011).
432   14.   Sims, J. E., Tunnacliffe, A., Smith, W. J. & Rabbitts, T. H. Complexity of
433   human T-cell antigen receptor beta-chain constant- and variable-region genes.
434   *Nature* **312,** 541–545 (1984).
435   15.   Tunnacliffe, A., Kefford, R., Milstein, C., Forster, A. & Rabbitts, T. H.
436   Sequence and evolution of the human T-cell antigen receptor beta-chain
437   genes. *Proc. Natl. Acad. Sci. U.S.A.* **82,** 5068–5072 (1985).
438   16.   Dickinson, A. M. *et al.* In situ dissection of the graft-versus-host activities of
439   cytotoxic T cells specific for minor histocompatibility antigens. *Nat. Med.* **8,**
440   410–414 (2002).
441   17.   Viney, J. L., Prosser, H. M., Hewitt, C. R., Lamb, J. R. & Owen, M. J.
442   Generation of monoclonal antibodies against a human T cell receptor beta
443   chain expressed in transgenic mice. *Hybridoma* **11,** 701–713 (1992).
444   18.   Reff, M. E. *et al.* Depletion of B cells in vivo by a chimeric mouse human
445   monoclonal antibody to CD20. *Blood* **83,** 435–445 (1994).
446   19.   Ricciardelli, I. *et al.* Towards gene therapy for EBV-associated posttransplant

447 lymphoma with genetically modified EBV-specific cytotoxic T cells. *Blood* **124,**
448 2514–2522 (2014).

449 20. Swerdlow, S. H., International Agency for Research on CancerWorld Health
450 Organization. *WHO Classification of Tumours of Haematopoietic and*
451 *Lymphoid Tissues.* (International Agency for Research on Cancer, 2008).

452 21. Pule, M. *et al.* A chimeric T cell antigen receptor that augments cytokine
453 release and supports clonal expansion of primary human T cells. *Molecular*
454 *Therapy* **12,** 933–941 (2005).

455 22. Philip, B. *et al.* A highly compact epitope-based marker/suicide gene for easier
456 and safer T-cell therapy. *Blood* **124,** 1277–1287 (2014).

457 23. Freeman, J. D., Warren, R. L., Webb, J. R., Nelson, B. H. & Holt, R. A.
458 Profiling the T-cell receptor beta-chain repertoire by massively parallel
459 sequencing. *Genome Research* **19,** 1817–1824 (2009).

460 24. Rosenberg, W. M., Moss, P. A. & Bell, J. I. Variation in human T cell receptor
461 V beta and J beta repertoire: analysis using anchor polymerase chain reaction.
462 *Eur. J. Immunol.* **22,** 541–549 (1992).

463 25. Brüggemann, M. *et al.* Powerful strategy for polymerase chain reaction-based
464 clonality assessment in T-cell malignancies Report of the BIOMED-2
465 Concerted Action BHM4 CT98-3936. *Leukemia* **21,** 215–221 (2006).

466 26. Stevenson, F. K. *et al.* Antibodies to shared idiotypes as agents for analysis
467 and therapy for human B cell tumors. *Blood* **68,** 430–436 (1986).

468 27. Hamblin, T. J. *et al.* Initial experience in treating human lymphoma with a
469 chimeric univalent derivative of monoclonal anti-idiotype antibody. *Blood* **69,**
470 790–797 (1987).

471 28. Ramos, C. A. *et al.* Clinical responses with T lymphocytes targeting
472 malignancy-associated κ light chains. *J. Clin. Invest.* **126,** 1–9 (2016).

473 29. Schulz, H. *et al.* Chemotherapy plus Rituximab versus chemotherapy alone for
474 B-cell non-Hodgkin's lymphoma. *Cochrane Database Syst Rev* CD003805
475 (2007). doi:10.1002/14651858.CD003805.pub2

476 30. Fang, C., Xu, W. & Li, J.-Y. A systematic review and meta-analysis of
477 rituximab-based immunochemotherapy for subtypes of diffuse large B cell
478 lymphoma. *Ann Hematol* **89,** 1107–1113 (2010).

479 31. Boyiadzis, M. *et al.* The Society for Immunotherapy of Cancer consensus
480 statement on immunotherapy for the treatment of hematologic malignancies:
481 multiple myeloma, lymphoma, and acute leukemia. *Journal for*
482 *ImmunoTherapy of Cancer* 1–25 (2016). doi:10.1186/s40425-016-0188-z

483 32. Davila, M. L. *et al.* Efficacy and toxicity management of 19-28z CAR T cell
484 therapy in B cell acute lymphoblastic leukemia. *Sci Transl Med* **6,** 224ra25–
485 224ra25 (2014).

486 33. Porter, D. L., Levine, B. L., Kalos, M., Bagg, A. & June, C. H. Chimeric antigen
487 receptor–modified T cells in chronic lymphoid leukemia. *N Engl J Med* **365,**
488 725–733 (2011).

489 34. Mamonkin, M., Rouce, R. H., Tashiro, H. & Brenner, M. K. A T-cell-directed
490 chimeric antigen receptor for the selective treatment of T-cell malignancies.
491 *Blood* **126,** 983–992 (2015).

492 35. Pinz, K. *et al.* Preclinical targeting of human T-cell malignancies using CD4-
493 specific chimeric antigen receptor (CAR)-engineered T cells. *Leukemia* **30,**
494 701–707 (2016).

495 36. Boulter, J. M. *et al.* Stable, soluble T-cell receptor molecules for crystallization
496 and therapeutics. *Protein Eng.* **16,** 707–711 (2003).

497 37. Garboczi, D. N. *et al.* Assembly, specific binding, and crystallization of a
498 human TCR-alphabeta with an antigenic Tax peptide from human T
499 lymphotropic virus type 1 and the class I MHC molecule HLA-A2. *J. Immunol.*
500 **157,** 5403–5410 (1996).

501 38. Wyer, J. R. *et al.* T cell receptor and coreceptor CD8 alphaalpha bind peptide-

502   MHC independently and with distinct kinetics. *Immunity* **10,** 219–225 (1999).
503   39.   Straathof, K. C. An inducible caspase 9 safety switch for T-cell therapy. *Blood*
504   **105,** 4247–4254 (2005).
505
506

507

508   **OUTLINE METHODS**

509

510   **Cell lines**

511

512   293T and K562 cell lines were cultured in IMDM (Lonza, Basel, Switzerland)

513   supplemented with 10% FBS (FBS, HyClone, GE, Buckinghamshire, UK) and 2 mM

514   GlutaMax (Invitrogen, CA, USA). Jurkat, Jurkat TCR-KO (and engineered variants),

515   HD-Mar2, HPB-ALL, H9, T-ALL1, MJ, CCRF-CEM and HH cells were cultured in

516   complete RPMI (RPMI1640, Lonza, Basel, Switzerland, supplemented with 10% FBS

517   and 2 mM GlutaMax). Cells were maintained in a humidified atmosphere containing

518   5% CO_2 at 37°C. All cell lines were routinely tested for mycoplasma and for surface

519   expression of target antigens. All cell lines were obtained from American Tissue

520   Culture Collection (ATCC), Deutsche Sammlung von Mikroorganismen und

521   Zellkulturen (DSMZ) or Public Heath England collections. Jurkat TCR-KO cells were a

522   kind gift from the laboratory of Prof Hans Stauss.

523

524

525   **Cloning, expression and purification of TCR protein.**

526

527   The C5861 TCR expressing a TRBC2 domain[36] and the ILA1 TCR expressing a

528   TRBC1 domain[37], constructed using a disulphide-linked construct, were used to

529   produce the soluble α- and β- chain domains (variable and constant) for each TCR.

530   The TCRα and TCRβ chains were inserted into separate pGMT7 expression plasmids

531   under the control of the T7 promoter. Competent Rosetta DE3 *E. Coli* cells (Merck,

532   Darmstadt, Germany) were used to produce the C5861 and ILA1 TCRs in the form of

533   inclusion bodies using 0.5M IPTG to induce expression. Soluble C5861 and ILA1

534   TCRs were refolded as previously described[36] purified by anion exchange (Poros

535   50HQ, Life Technologies, Cheshire, UK) and size exclusion chromatography (S200

536   GR, GE Healthcare, Buckinghamshire, U.K.).

537

538   **Surface Plasmon Resonance (SPR) analysis**

539

540   The binding analysis was performed using a Biacore T200 (GE Healthcare,

541   Buckinghamshire, UK) equipped with a CM5 sensor chip as previously reported[38].

542   Briefly, 500-1000 Response Units (RUs) of JOVI-1 antibody was linked by amine

543   coupling to the chip surface. For the C5861 TRBC2 TCR, ten serial dilutions were

544   injected over the immobilised JOVI-1 and equibilibrium binding analysis was

545 performed. The equilibrium-binding constant (K_D (E)) values were calculated using a

546 nonlinear curve fit ($y = (P1x)/(P2+x)$). For the ILA1 TRBC1 TCR, single kinetic

547 injections were performed. For kinetics analysis, the K_{on} and K_{off} values were

548 calculated assuming 1:1 Langmuir binding and the data were analysed using a global

549 fit algorithm (BIAevaluation 3.1™).

550

551 **Cell staining and flow cytometry**

552

553 Flow cytometry was performed using BD LSR Fortessa instrument (BD, NJ, USA).

554 FACS sorting was performed using BD FACSAria (BD, NJ, USA). Staining steps were

555 performed at room temperature for 20 minutes, with PBS washes between steps. For

556 staining of intracellular antigens cells were fixed and permeabilised with 100uL of

557 Cytofix/ Cytoperm (BD, NJ, USA) for 5 minutes prior to staining, and wash steps were

558 performed using PermWash (BD, NJ, USA). The following antibodies were used (all

559 anti-human unless otherwise specified, clone identity in brackets): CD2 (TS1/8), CD3

560 (UCHT1), CD4 (OKT4), CD5 (UCHT2), CD7 (CD7-6B7), CD8 (SK1), human/ murine

561 CD11b (M1/70), CD14 (M5E2), CD19 (HIB19), CD25 (BC96), CD45 (HI30), CD45RA

562 (HI100), CD56 (HCD56), CD57 (HCD57), CCR7 (GO43H7), TCR α/β (T10B9), all from

563 Biolegend, San Diego, CA, USA; CD34 (Qbend10, Miltenyi, Bergisch Gladbach,

564 Germany); TRBC1 (JOVI-1, Ansell, Bayport, MN, USA), fixable viability dye

565 (eBioscience, ThermoFisher, Waltham, MA, USA). Anti-TRBC1 CAR expression was

566 detected by staining for RQR8 marker gene[22] with anti-CD34, or anti-MuFab (115-

567 116-072, Jackson Immuno, Westgrove, PA, USA). All antibodies other than JOVI-1

568 were validated by manufacturer for diagnostic use. At least 5000 target events were

569 acquired per sample. Analyses were conducted using FlowJo v10 (Treestar, Ashland,

570 OR, USA).

571

572

573 **Normal donors and viral peptide stimulation assays**

574

575 Approval for this study was obtained from the National Research Ethics Service,

576 Research Ethics Committee 4 (REC Reference number 09/H0715/64). All normal

577 donors provided informed consent.

578

579 PBMCs from unselected heathy donors were isolated by Ficoll-Paque (GE Healthcare,

580 Buckinghamshire, UK) gradient centrifugation were resuspended at 2 x 10^6 cells/ml

581 in 1ml complete media in wells of a 24-well plate. Overlapping peptide pools (15-mer,

582   11-mer overlap) derived from commonly immunogenic viral proteins were obtained

583   from JPT Technologies (Berlin, Germany, USA). The viruses investigated (protein

584   antigens in brackets) were cytomegalovirus, CMV (PP65) and adenovirus, AdV (hexon

585   and penton). Peptide pools were supplied as dried pellets containing 25ug/peptide and

586   were reconstituted in 50uL DMSO. To obtain a final concentration of 1ug/peptide/ml,

587   2ul of each peptide pool was added to each well of PBMCs.

588

589   After 1hr initial incubation, brefeldin A (BD, NJ, USA) was added to prevent Golgi

590   transport. After a further 14hrs of culture, the cells were washed and surface staining

591   was performed for viability, CD4 and CD8. The cells were then washed and lysed/

592   permeabilised, then stained for intracellular interferon-γ, CD3 and JOVI-1 before

593   resuspension for FACS analysis. Negative control peptide pool (actin, a ubiquitous

594   cytoskeletal protein) and positive control (PMA/ ionomycin, Sigma Aldrich, Darmstadt,

595   Germany) conditions were included. Low-frequency viral-specific T-cells were

596   identified by intracellular interferon-gamma expression, with positive response

597   threshold set as >0.01% above negative control staining.

598

599   **Identification of T-cell diiferentiation subsets and mucosal-associated invariate**

600   **T-cells (MAITs) in normal donor peripheral blood**

601

602   Cells were defined as: naïve (CD45RA+CD45RO-CCR7-CD62L-), central memory

603   (CD45RA-CD45RO+CCR7+CD62L+), effector memory (CD45RA-CD45RO+CCR7-

604   CD62L-) and effector (CD45RA-CD45RO+CCR7+CD62L+) and T-regulatory cells

605   (CD4+FOXP3+CD25+). MAITs were identified as CD3+CD8+CD4-CD161+TCR-

606   Vα7.2 +ve.

607

608   **Invariant Natural Killer T-cell (iNKT) isolation**

609

610   Peripheral blood mononuclear cells (PBMC) were isolated from healthy donor blood

611   bags (Welsh Blood Service) using standard density gradient centrifugation. iNKT cells

612   were purified from PBMC by magnetic separation using anti-iNKT TCR beads (Miltenyi

613   Biotec) according to manufacturer's recommendations. The purified cell fraction was

614   subsequently expanded with phytohaemagglutinin and allogeneic irradiated feeders

615   from three donors. After a minimum of 14 days post expansion, cells were phenotyped

616   and used in functional assays.

617

618   Molt-3 cell line (endogenously expressing CD1d) was pulsed overnight with 100 ng/ml

619   α-galactosylceramide (αGalCer, Sigma). iNKT lines were subsequently co-incubated

620   with Molt-3 pulsed with αGalCer for 5 hours in presence of monensin, brefeldin A and

621   CD107a antibody (all from BD Biosciences), according to manufacturer's

622   recommendations. iNKT lines were also incubated with media only, and with Molt-3

623   pulsed with vehicle only (DMSO). iNKTs were identified by upregulation of CD107a

624   and IFN-γ in response to Molt-3 pulsed with αGalCer.

625

626

627   **Retroviral transduction of T-cells**

628

629   RD114-pseudotyped supernatant was generated as follows: 293T cells were

630   transfected with vector plasmid; RDF, an expression plasmid to supply RD114

631   envelope (gift of Mary Collins, University College London); and PeqPam-env, a gagpol

632   expression plasmid (gift of Elio Vanin, Baylor College of Medicine). Transfection was

633   facilitated using Genejuice (Merck, Darmstad, Germany). Peripheral blood

634   mononuclear cell transductions were performed as follows: T cells from normal donors

635   were isolated by Ficoll (GE, Buckinghamshire, UK) gradient centrifugation and

636   stimulated with phytohemagglutinin (Sigma Aldrich, Darmstadt, Germany) at 5mg/mL.

637   Interleukin-2 (IL-2, Genscript, Nanjing, China) stimulation (100 IU/mL) was added

638   following overnight stimulation. On day 3, T cells were harvested, plated on retronectin

639   (Takara, Nojihigashi, Japan) and retroviral supernatant, and centrifuged at 1000g for

640   40 minutes. Transduction efficiency was determined on D6-7 following initial harvest

641   and further experiments were commenced on D7-10 following initial harvest. PBMCs

642   were maintained in complete RPMI.

643

644   **Generation and cytotoxicity assessment of EBV-specific CTLs**

645

646   This was performed as previously described[19]. Briefly, PBMCs from a normal donor

647   were infected with EBV resulting in B-cell transformation to produce immortalised

648   lymphoblastoid cells. These cells were irradiated and used as target cells to stimulate

649   untransfomed PBMCs from the same donor, selectively expanding EBV-specific CTLs

650   over a 23-day period. Cytotoxicity of EBV-CTLs against K562 cell line (an

651   erythroleukaemia cell line with loss of MHC class 1 expression), allogeneic and

652   autologous lymphoblastoid cells was assessed using standard 4hr chromium release

653   cytotoxicity assays as previously described[39].

654

655

656   **Preparation and staining of primary tumour samples for FACS or**

657   **immunohistochemistry**

658

659   Approval for this study was obtained from the National Research Ethics Service,

660   Research Ethics Committee 4 (REC Reference number 09/H0715/64). Informed

661   consent was obtained from all patients. For FACS, PBMCs from patients with T-cell

662   malignancies were obtained from whole blood or marrow samples by Ficoll-Paque (GE

663   Healthcare, Buckinghamshire, UK) gradient centrifugation prior to staining and

664   analysis as above. Gating strategies to identify tumour and healthy T-cells were

665   determined on a patient-specific basis according to data previously obtained by

666   primary clinical laboratories. For immunohistochemistry, fresh biopsy samples of

667   patients with a range of T-cell malignancies (see Figure 3f) were snap-frozen in liquid

668   nitrogen and tissue sections were prepared according to standard methodology. The

669   investigated antibodies included the mouse monoclonal anti-T Cell Receptor Beta 1

670   (clone JOVI.1; Ancell Corporation, Bayport, MN, USA) and the mouse monoclonal anti-

671   TCR beta F1 (clone 8A3; Thermo Fisher Scientific, Loughborough, UK). The

672   antibodies were assessed under different conditions (i.e. dilution and antigen retrieval

673   protocol) and the chosen dilution which showed selective background-free reaction in

674   fresh tissue sections of human reactive tonsils (nr. 2) used as positive control were

675   1:5000 for JOVI.1 and 1:50 for TCR Beta F1 respectively. The staining procedure was

676   performed using the Roche-Ventana BenchMark Ultra autostainer (Ventana Medical

677   System, Tuscon, US). Counterstaining was performed using haematoxylin and bluing

678   reagent from Ventana/Roche; slides were mounted with cover slips and air-dried.

679

680

681   **Chromium release cytotoxicity assays**

682

683   Standard 4hr chromium release cytotoxicity assays were performed as previously

684   described[39], with all assays performed in triplicate. NK cell depletion was performed

685   prior to assays using CD56 magnetic bead depletion and LD columns (Miltenyi,

686   Begisch Gladbach, Germany).

687

688   **FACS-based co-culture and cytotoxicity assays**

689

690   Target and effector cells were resuspended at 1M cells/ml in complete media. 50-

691   100uL of each cell suspension was added to wells of a V-bottom 96-well plate to

692   achieve a 1:1 E:T ratio with 50 000 or 100 000 targets/ well. For some experiments

693   target cell were pre-labelled with carboxyfluorescein succinimidyl ester (CFSE) or

694   CellTrace Violet (CTV, both Invitrogen, Carlsbad, CA, USA) dyes according to

695   manufacturer's instructions. The plate was placed in a standard cell culture incubator

696   containing 5% CO_2 at 37°C. After 24hrs the plate was spun down at 400G for 5mins,

697   100uL of supernatant was removed for cytokine assays and replaced with fresh

698   complete media. At 48hrs or 7 days, the plate was spun down at 400G for 5mins and

699   supernatant was decanted. 100uL of staining cocktail (appropriate antibodies/ viability

700   dye (eBioscience, ThermoFisher, Waltham, MA, USA) diluted in PBS) was added and

701   cells were stained for 20mins in the dark at room temperature. Wells were then

702   washed with a further 100uL of PBS and spun down at 400G for 5 mins. Supernatant

703   was decanted. Counting beads (Flow check fluorospheres, BD, NJ, USA) were

704   washed in PBS then resuspended at 100 000 beads/ ml in PBS. 100uL of PBS/

705   counting bead mixture was added to each cells (10 000 beads/ well). 2000 beads were

706   acquired per sample. Gating on single live target cells was performed according to

707   exclusion of fixable viability dye, forward and side scatter characteristics and

708   expression of fluorescent protein, marker gene or fluorescent dye. Assays were

709   performed in triplicate. % cytotoxicity was calculated as: 10000/ number of beads

710   collected x number of target cells at end/ number of target cells at start of culture x

711   100.

712

713   For primary tumour killing experiments, allogeneic or autologous T-cells were used,

714   depending on the availability of cryopreserved normal patient T-cells. Bespoke gating

715   strategies were used to identify normal and malignant T-cells in each patient sample.

716

717   **Cell sorting with magnetic bead selection**

718

719   Transduced T-cells positive or negative for the RQR8 marker gene (contains

720   Qbend10-CD34 epitope) were selected by positive or negative bead selection

721   according to the manufacturer' instructions (Miltenyi, Miltenyi, Bergisch Gladbach,

722   Germany) using MS or LD columns respectively. For TRBC1 T-cell positive or negative

723   selection, cells were initially stained with JOVI-1-biotin then incubated with

724   streptavidin-conjugated magnetic beads, then separated according to the

725   manufacturer's instructions. To increase purity a second selection/ depletion round

726   was performed.

727

728   **Murine models of T-cell malignancy**

729

730   This work was performed under United Kingdom home-office–approved project license

731   and was approved by University College London Biological Services Ethical Review

732   Committee. 6-8 week old male non-obese diabetic-severe combined

733   immunodeficiency γ-chain–deficient (NSG) mice (Jackson Laboratory, Bar Harbor,

734   ME, USA) were intravenously injected via the tail vein with tumour cells, human

735   PBMCs or CAR T-cells as described in the text. An otherwise identical irrelevant

736   control CAR targeting B-cell maturation antigen, which is not expressed in T-cell

737   malignancies, was used in some experiments as indicated in the text. Tail vein bleeds

738   of 50uL were undertaken as indicated in the text. At the time of cull, in some

739   experiments bone marrow was harvested. Single cell suspensions were prepared and

740   analysed for presence of T-cells and residual tumour by flow cytometry. Tumour cells

741   were identified by CD19 or BFP marker gene according to experiment. CAR T-cells

742   were identified by expression of RQR8 marker gene.

743

744   For experiments with a survival endpoint or engraftment of PBMCs, mice were

745   monitored with at least twice weekly weighing. Animals with >10% weight loss or those

746   displaying evidence of GvHD or tumour progression including hunched posture, poor

747   coat condition, reduced mobility, pilorection or hind limb paralysis were culled.

748

749   Bioluminescent imaging of mice was performed using IVIS system (Perkin Elmer,

750   Buckinghamshire, UK). Prior to imaging, animals were placed in an anesthetic

751   chamber. General anesthesia was induced using inhaled isoflurane. Following

752   induction, intraperitoneal injection of luciferin (200uL via 27G needle) was undertaken.

753   After 2 minutes, mice were placed in the imaging chamber. Simultaneous optical and

754   bioluminescent imaging was performed. Anaesthesia was maintained by continued

755   inhalation of isoflurane during imaging.

756

757   **Statistical analyses**

758

759   Unless otherwise noted, data are summarised as mean $\pm$ SEM. Student's *t*-test was

760   used to determine statistically significant differences between samples for normally

761   distributed variables, with Mann-Whitney U-test used for non-parametrically distributed

762   variables. $p < 0.05$ (2-tailed) indicated a significant difference. Unless otherwise stated,

763   variances were similar between study populations. When variances were unequal,

764   Welch's correction for unequal variance was used. Paired analyses were used when

765 appropriate. When 3 groups were compared, 1-way ANOVA with Dunnett's test for

766 multiple comparisons with alpha of 0.05 were used. When multiple t-tests were

767 performed, statistical significance was determined using the Holm-Sidak method with

768 alpha of 0.05. Neither randomisation nor blinding was done during the *in vivo* study.

769 However, mice were matched based on the tumor signal for control and treatment

770 groups before infusion of control or gene-modified T-cells. Cohort sizes were based

771 on number required to demonstrate 90% reduction in tumour bioluminescence, 95%

772 confidence with 80% power. Survival curves were generated using the Kaplan-Meier

773 method with hazard ratios calculated by Mantel-Haenszel method. All animal studies

774 were performed at least twice, with data presented representing one representative

775 experiment. Graph generation and statistical analyses were performed using Prism

776 version 7.0b software (GraphPad, La Jolla, CA, USA).

777

778

779

780

781

782

783

784

785

786

787

788

789

790

791
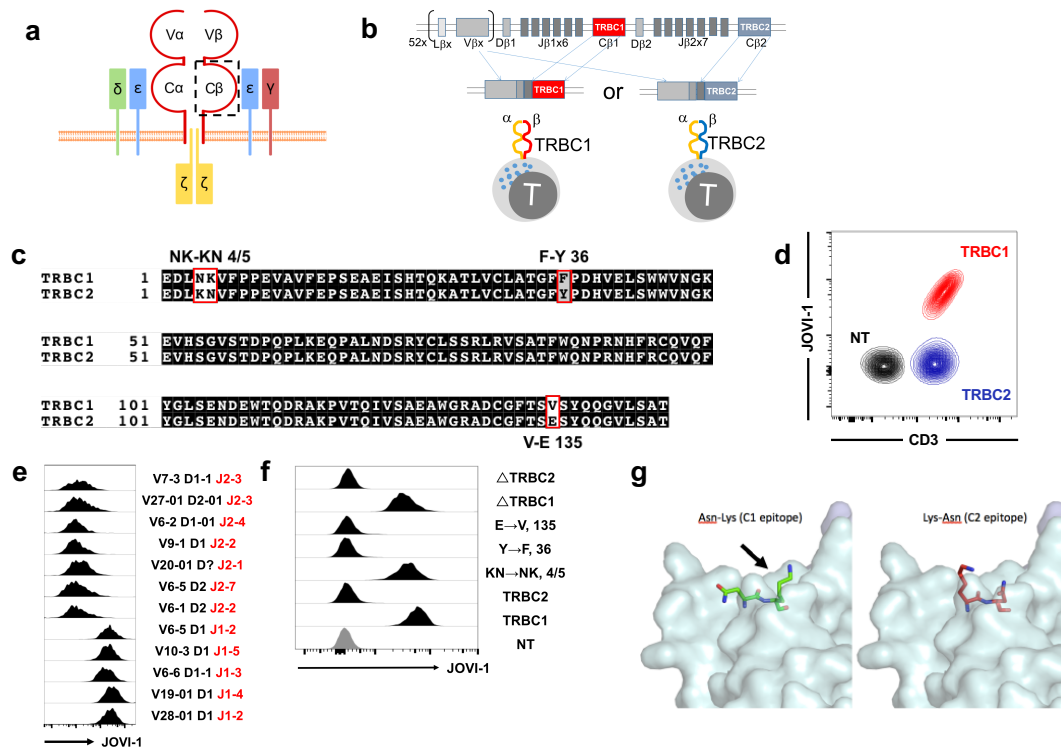
Figure 1: During T-cell receptor gene re-arrangement, each T-cell selects either TRBC1 or TRBC2, which can be specifically differentiated using an antibody. (a) Proposed structure of the TCR-CD3 complex assembled on T-cell surface (beta constant region highlighted) (b) The process of beta gene arrangement involving specific VDJ recombination (c) Alignment of TRBC1 and TRBC2 protein sequences, differences highlighted in red (d) Staining of non-transduced and engineered TRBC1-JKO, TRBC2-JKO cell lines with CD3 and JOVI-1 antibodies (e) JOVI-1 staining of 293T cells, transfected to express TCRs with varying specificities and TRBJ usage (gated on CD3+ cells) (f) JOVI-1 staining of engineered cell lines with each difference between TRBC1 and TRBC2 introduced individually (g) 3D representation of TRBC1 and TRBC2 epitopes on the surface of TRBC. TCR = T-cell receptor; VDJ = variable, diversity, joining; JKO = Jurkat T-Cell receptor knockout. TRBC = T-cell receptor beta constant.
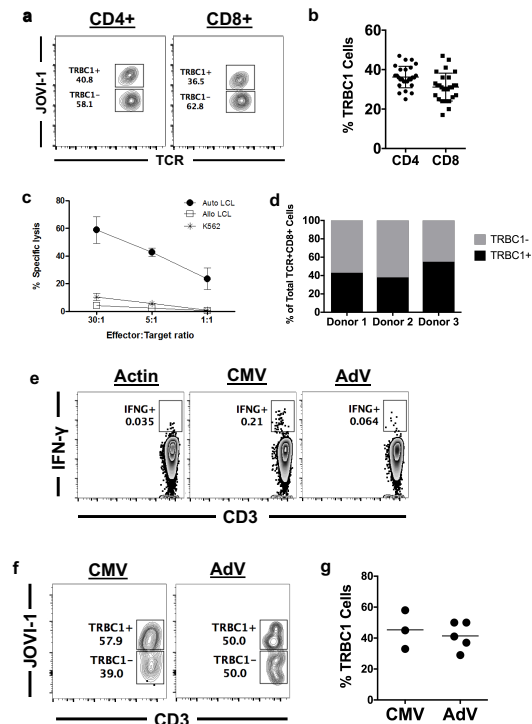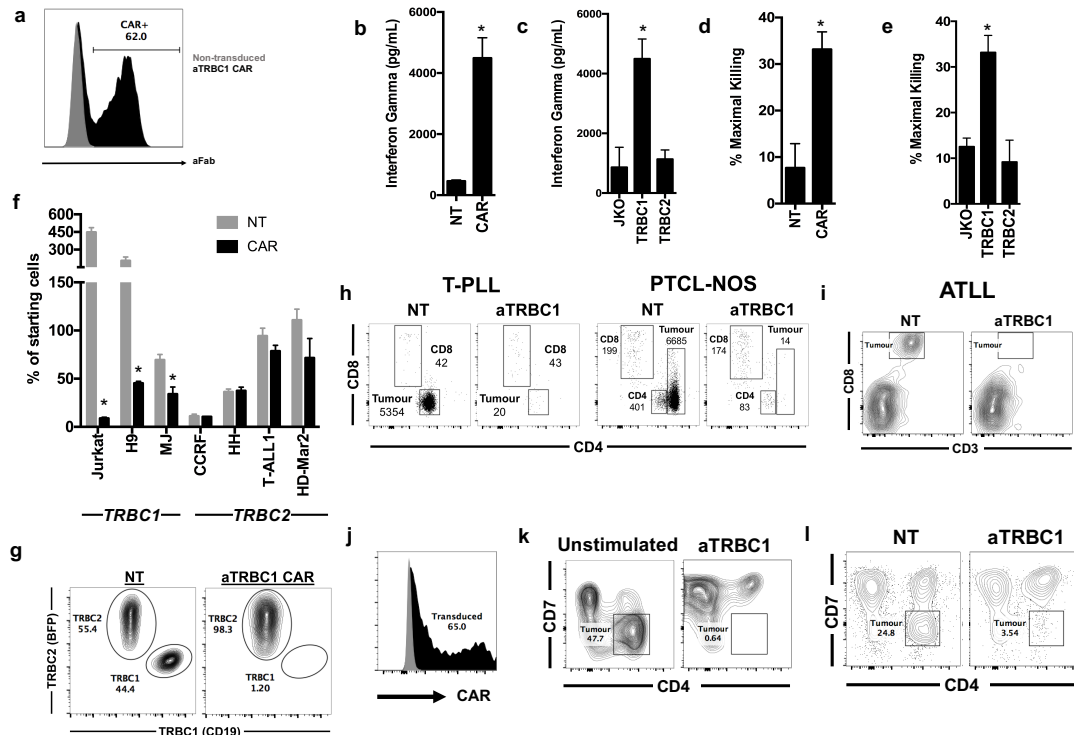
814
815
816 **Figure 2:** Unselected polyclonal and viral-specific T-cells contain both TRBC1+ and
817 TRBC1- populations. (a) Staining of sample normal donor CD4 (left) and CD8 (right)
818 T-cells with pan-TCR and JOVI-1 antibodies (b) Proportion of normal T-cells
819 expressing TRBC1 in CD4 and CD8 compartments, data from 27 normal donors. (c)
820 Killing of cell lines by EBV-CTLs, measured by 4hr chromium release assay (d)
821 TRBC1+/TRBC1- proportion of EBV-CTLs in 3 normal donors (e) Identification of CMV
822 or AdV-specific T-cells by IFN-G staining after peptide stimulation, data from
823 representative donor (f) Staining of viral specific T-cells with CD3 and JOVI-1 (gated
824 on cells as identified in e) (g) TRBC1 expression in viral specific cells, summary data
825 from 3 (CMV) and 5 (AdV) normal donors. TCR = T-cell receptor, EBV = Epstein Barr
826 virus, CTL = cytotoxic T-lymphocyte, CMV = cytomegalovirus, AdV = adenovirus, IFN-
827 G = interferon gamma.
828
829
830
831
832
833
834
835

836
837
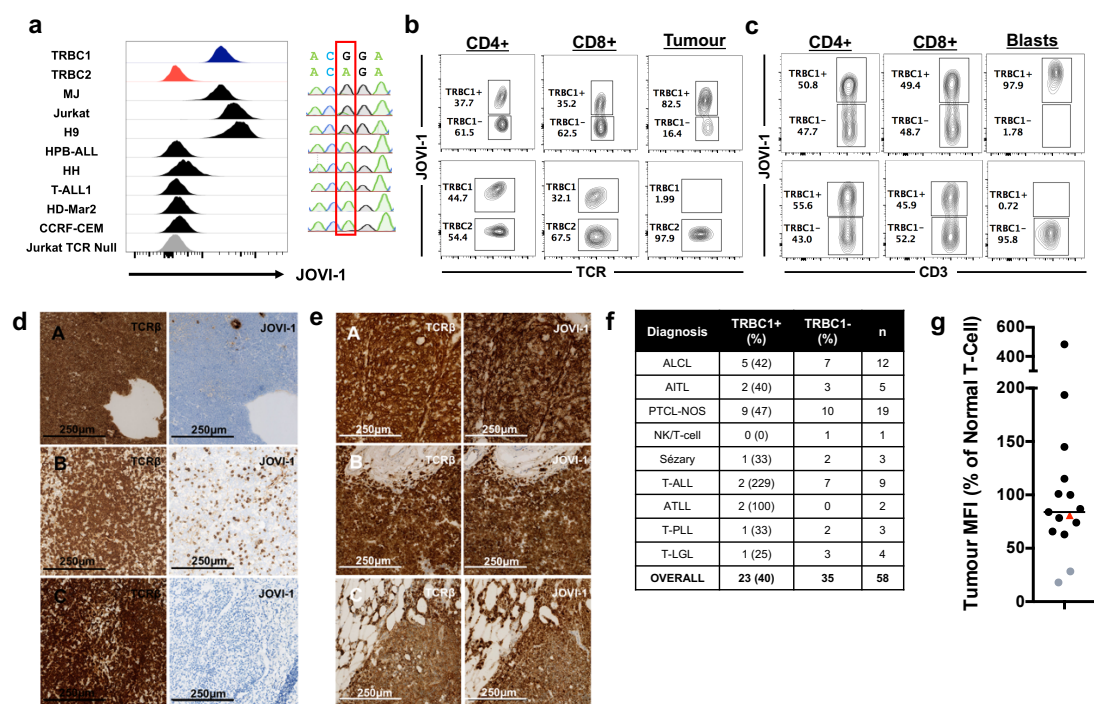
Figure 3: T-cell-derived cell lines and primary T-cell malignancies are clonally TRBC1+ or TRBC1-. (a) Staining of cell lines with JOVI-1 (left panel), gated on CD3+ cells with matched Sanger sequencing traces of TCR-beta constant region (right panel) (b) Staining of normal and malignant T-cells from 2 representative patients with T-LGL, assessed by flow cytometry. Top panel shows TRBC1+ tumour, bottom panel shows TRBC1- tumour. Tumour gating = TCR+CD4-CD8+CD57+ Small numbers of TRBC1- cells in tope panel 'tumour' gate likely reflect normal CD8+CD57+ T-cells, clonality suggested by abnormal TRBC1+:TRBC1- ratio (c) Staining of normal and malignant T-cells from 2 representative patients with T-ALL, assessed by flow cytometry. Top panel shows TRBC1+ tumour, bottom panel shows TRBC1- tumour. Tumour gating = CD3(intra)+CD4+CD8+. (d) Staining of frozen tissue sections of 3 cases of TCR+ TRBC1- lymphoma with TCR (left panel) and JOVI-1 (right panel). Positive cells stain brown. Small numbers of admixed polyclonal TRBC1+ T-cells are typically seen. Tumour histology: A = T-acute lymphoblastic leukaemia (T-ALL), B = angioimmunoblastic T-cell lymphoma (AITL), C = AITL (e) Staining of frozen tissue sections of 3 cases of TCR+ TRBC1+ lymphoma with TCR (left panel) and JOVI-1 (right panel). Positive cells stain brown. A = anaplastic large cell lymphoma (ALCL), B = T-ALL, C = peripheral T-cell lymphoma not otherwise specified (PTCL-NOS) (f) Summary data of TRBC1 expression in primary samples of TCR+ malignancies. (g) TCR expression on tumour cells and TRBC1+ cell lines. Tumour expression of TCR

858   was quantified by MFI on FACS, and is expressed as a percentage of TCR expression
859   on admixed normal T-cells from the same patient. Grey triangles represent cases of
860   ATLL, with other histologies represented by black circles. Red triangle = Jurkat cell
861   line. T-LGL = T-large granular lymphocytosis, T-ALL = T-acute lymphoblastic
862   leukaemia, AITL = angioimmunoblastic lymphoma, ALCL = anaplastic large cell
863   lymphoma, NK = natural killer, ATLL = adult T-cell leukaemia/ lymphoma, T-PLL = T-
864   prolymphocytic leukaemia. MFI = median fluorescence intensity.
865
866
867
868
869
870
871
872
873
874
875
876
877
878
879
880
881
882
883
884
885
886
887
888
889
890
891
892
893
894

895
896

Figure 4: Anti-TRBC1 CART-cells demonstrate efficacy and specificity against TRBC1+ tumours *in vitro*. (a) Example transduction shows anti-TRBC1 CAR expression on surface of transduced T-cells. (b) Interferon gamma release by NT or anti-TRBC1 CAR T-cells against TRBC1-JKO cells, 24-hour co-culture. (c) Interferon gamma release by anti-TRBC1 CAR T-cells against NT-JKO, TRBC1-JKO or TRBC2-JKO cells, 24-hour co-culture. (d) Killing of TRBC1-JKO cells by NT or anti-TRBC1 CART-cells, 4hr chromium release assay. *p<0.01 for comparison v NT effectors. (e) Killing of TRBC1-JKO or TRBC2-JKO cells by anti-TRBC1 CART-cells, 4hr chromium release assay *p<0.01 for comparison v JKO-NT target cells. (f) Flow-based cytotoxicity assay, target cell numbers expressed as % of starting cells after 48hrs. (g) Co-culture of mixed TRBC1/ TRBC2 cells, example FACS plot at 48hrs. (h) Primary T-cell malignant samples with admixed normal CD8 T-cells after 120hr co-culture with NT or anti-TRBC1 allogeneic CAR –cells. Left panel = case of T-PLL, tumour cells were CD7bright CD4+. There were no normal CD4 cells but normal CD8 cells were present. Right panel = PTCL-NOS. Numbers represent % of events. Tumour cells were CD4brightCD7-. Normal admixed CD4 and CD8 cells were present. Numbers represent absolute numbers of events. (i) Primary ATLL sample after 72hr co-culture with allogeneic NT or anti-TRBC1 CAR T-cells. Tumour cells were CD3dimCD8+CD7-. Numbers represent % of events. (j) Transduction of PBMCs from patient with ATLL, assessed by RQR8 marker gene. Grey = NT cells, black = anti-TRBC1. (k) Tumour

917 burden following transduction with anti-TRBC1 CAR. (l) Primary ATLL sample after
918 72hr co-culture with autologous NT or anti-TRBC1 T-cells. Tumour gating =
919 CD2+CD4+CD7-CD8-. All experiments other than in j-l used effector T-cells from
920 normal healthy donors. NT = non-transduced, JKO = Jurkat T-cell receptor-null, CAR
921 = chimeric antigen receptor, BFP = blue fluorescent protein, ATLL = adult T-cell
922 leukaemia/ lymphoma, T-PLL = T-prolymphocytic leukaemia, PTCL-NOS = peripheral
923 T-cell lymphoma, not otherwise specified.
924
925
926
927
928
929
930
931
932
933
934
935
936
937
938
939
940
941
942
943
944
945
946
947
948
949
950
951
952
953

954

955

956

957

958
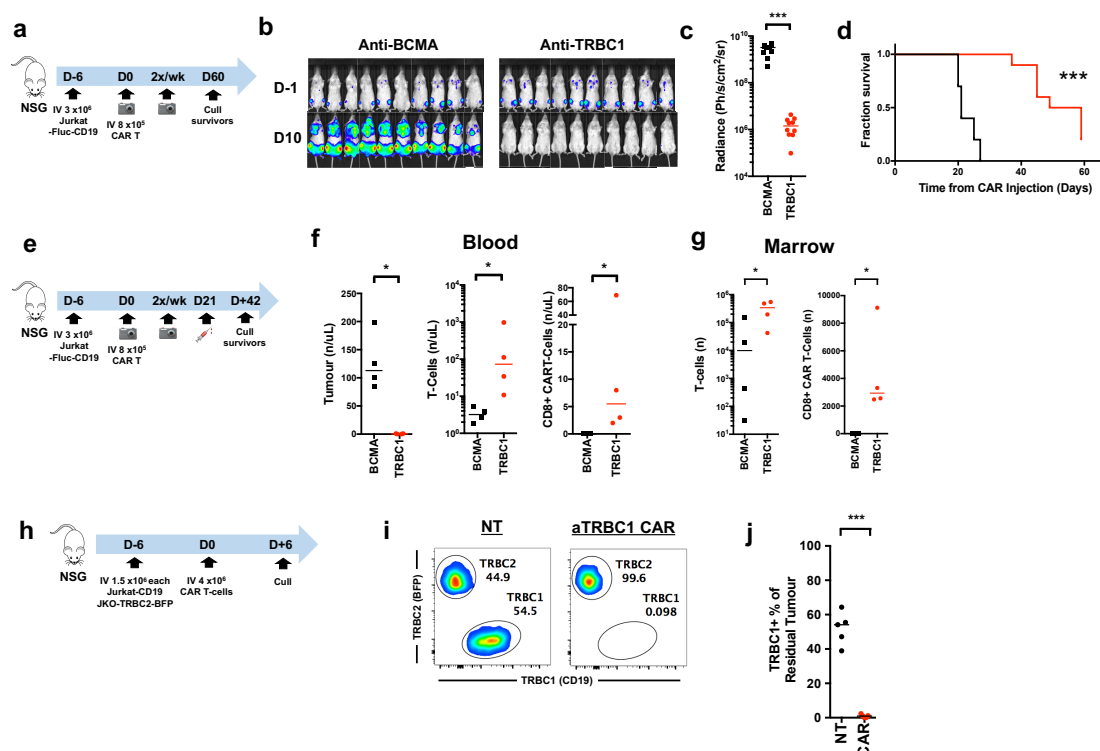
Figure 5: Efficacy and specificity of anti-TRBC1 CAR in murine models of TRBC1+ malignancy. (a) Flow diagram of Jurkat survival experiment (b) Bioluminescence imaging at D-1 and D10 following CAR injection (c) Radiance of individual animals at D10 following CAR injection, compared via Student's t-test (d) Survival curve of animals in Jurkat experiment (median OS 54 v 21 days, HR = 0.037, p < 0.00001, n = 10/ group) (e) Flow diagram of Jurkat persistence experiment (f) Jurkat tumour, total T-cell and CD8 CAR-T cell numbers from bleed at D21 following CAR injection (g) Numbers of total T-cells and CD8 CAR T-cells in marrow at time of cull (D42 in anti-TRBC1 CAR recipients). Comparisons in f,g were made using Mann-Whitney U-test. CAR was detected by expression of RQR8 marker gene (h) Flow diagram of specificity experiment (i) Flow cytometry of bone marrow in NSG mice engrafted with equal proportions of TRBC1-Jurkat or TRBC2-JKO cells following treatment with NT effectors or anti-TRBC1 CART-cells, representative examples. TRBC1 cells were detected by CD19 marker gene, TRBC2 cells were detected by BFP marker gene) Quantification of TRBC1 proportion of residual Jurkat tumour by flow cytometry, individual values shown. All experiments used effector T-cells from normal healthy donors. Comparison by Student's t-test. Horizontal lines represent median values.

978

979

980

981
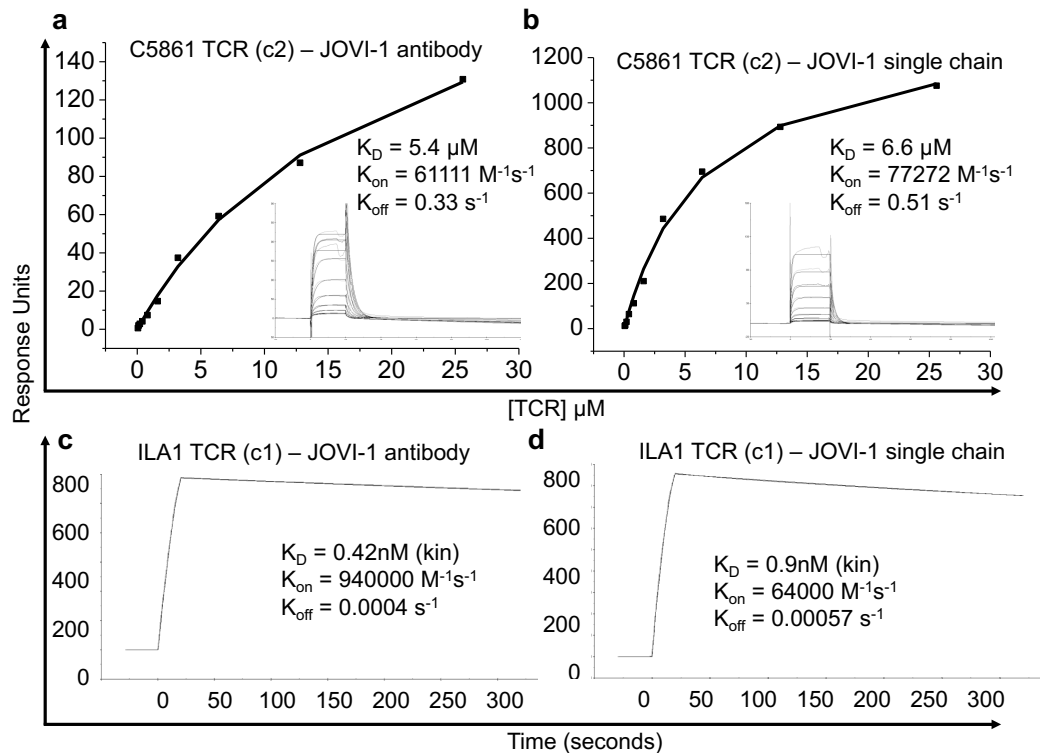
982 **Supplementary Figure 1**: Surface plasmon resonance data of JOVI-1 binding to
983 TRBC1 and TRBC2 TCR protein. JOVI-1 antibody (a) and single chain variable
984 fragment (ScFv) (b) binding to C5861 (TRBC2) TCR protein. JOVI-1 antibody binding
985 (c) and ScFv binding (d) to ILA1 (TRBC1) TCR. TCR = T-cell receptor, ScFv = single
986 chain variable fragment. Top row = plots demonstrating TCR concentration v peak
987 response units for binding to TRBC2 TCR, with time v response units plots at varying
988 concentrations of TCR inset. Bottom row demonstrates time v response units plots for
989 binding to TRBC1 TCR.

990

991

992

993

994

995

996

997

998
999
1000
1001

1002
1003
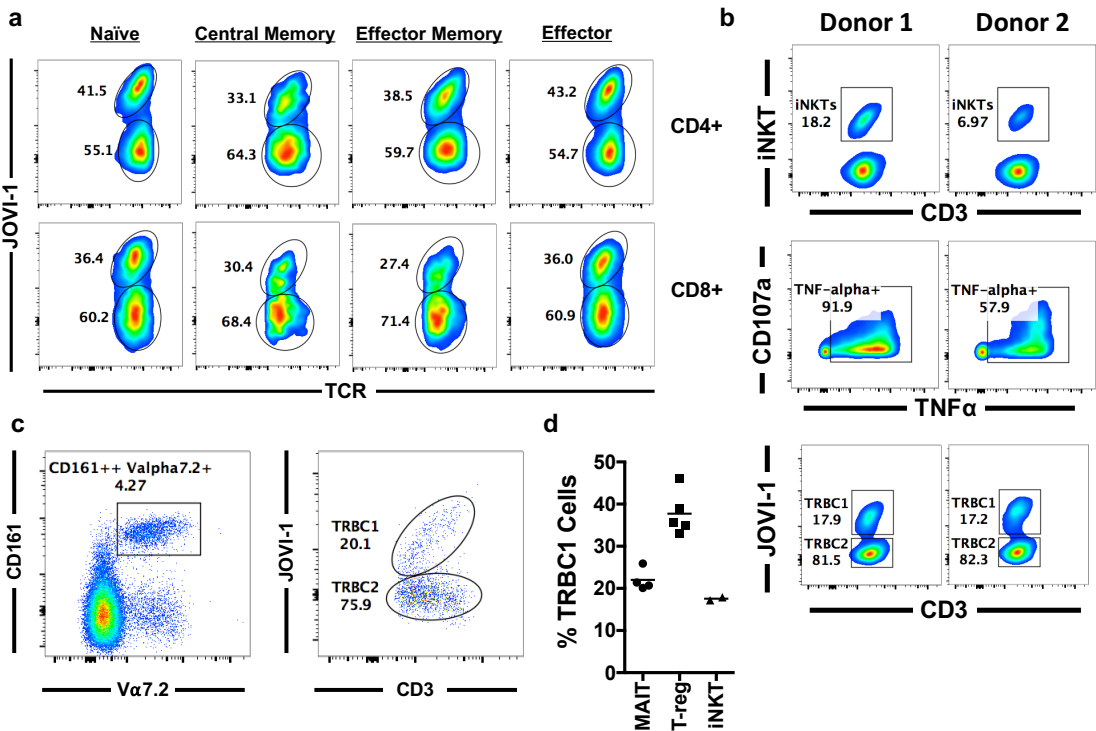
1004 **Supplementary Figure 2:** TRBC1 expression in T-cell subsets. (a) Naïve
1005 (CD45RA+CD45RO-CCR7-CD62L-), central memory (CD45RA-
1006 CD45RO+CCR7+CD62L+), effector memory (CD45RA-CD45RO+CCR7-CD62L-)
1007 and effector (CD45RA-CD45RO+CCR7+CD62L+) were identified by FACS. Staining
1008 with TCR and JOVI-1 antibodies demonstrated each T-cell population contained both
1009 TRBC1+ and TRBC1- cells. Data from 1 donor shown, repeated in 4 donors. (b) iNKT
1010 cell lines were produced as described in Methods section. Cells were
1011 CD3+Valpha24Jalpha18+ (top row) and expressed TNF-alpha and CD107a in
1012 response to Molt-3 cells pulsed with αGalCer (middle row, gated on iNKTs). Cells
1013 expressed both TRBC1+ and TRBC1- TCRs (bottom row, gated on iNKTs). (c) MAITs
1014 were identified as CD3+CD8+CD161brightValpha7.2 cells (left panel) and contained
1015 both TRBC1 and TRBC2 cells (right panel) (d) Summary data of TRBC1 expression in
1016 T-cell populations. TCR = T-cell receptor, MAIT = mucosal-associated invariant T-
1017 cells, iNKT = invariant natural killer/ T-cells.

1018
1019

1020

1021

1022

1023

1024

1025
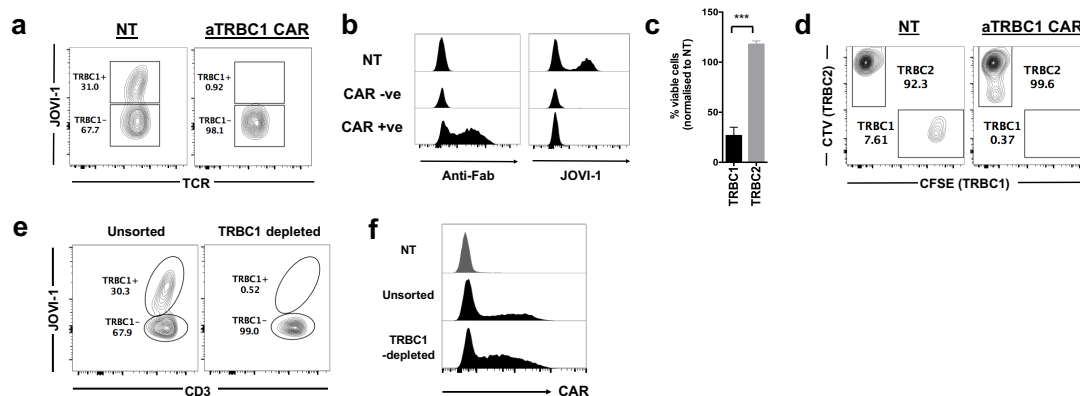
Supplementary Figure 3: Epitope blocking and primary T-cell cytotoxicity assay using anti-TRBC1 CAR. a) NT cells (left) and anti-TRBC1 CAR-transduced cells (right) stained with TCR and JOVI-1 antibodies, representative example, donor n > 10. b) Anti-TRBC1 CAR T-cells sorted into CAR-ve and CAR +ve fractions by CD34 magnetic sort, stained with anti-murine Fab antibody (left panel) or JOVI-1 antibody (right panel). Representative example, repeated x 3 c) Killing of fluorescently labelled primary TRBC1 or TRBC2 T-cells in 1:1 co-culture with autologous non-transduced or anti-TRBC1 CART-cells, FACS at 7 days, n = 3, ***p<0.001, unpaired t-test anti-TRBC1 CAR v NT effectors. d) Co-culture with CFSE-labelled TRBC1 and CTV-labelled TRBC2 cells, mixed at 1:2 ratio and incubated with autologous NT or anti-TRBC1 CAR T-cells, flow cytoemetry at 7 days, 1 representative donor shown, donor n = 3. e) Example of purity of TRBC1-depleted T-cells f) Transduction of unsorted or TRBC1-depleted T-cells with anti-TRBC1 CAR, transduction assessed by blue fluorescent protein marker gene. 1 representative donor shown, repeated in >3 donors. All experiments used T-cells from normal healthy donors. NT = non-transduced, CAR = chimeric antigen receptor, CFSE = carboxyfluorescein, CTV = Cell Trace Violet

1042

1043

1044

1045

1046
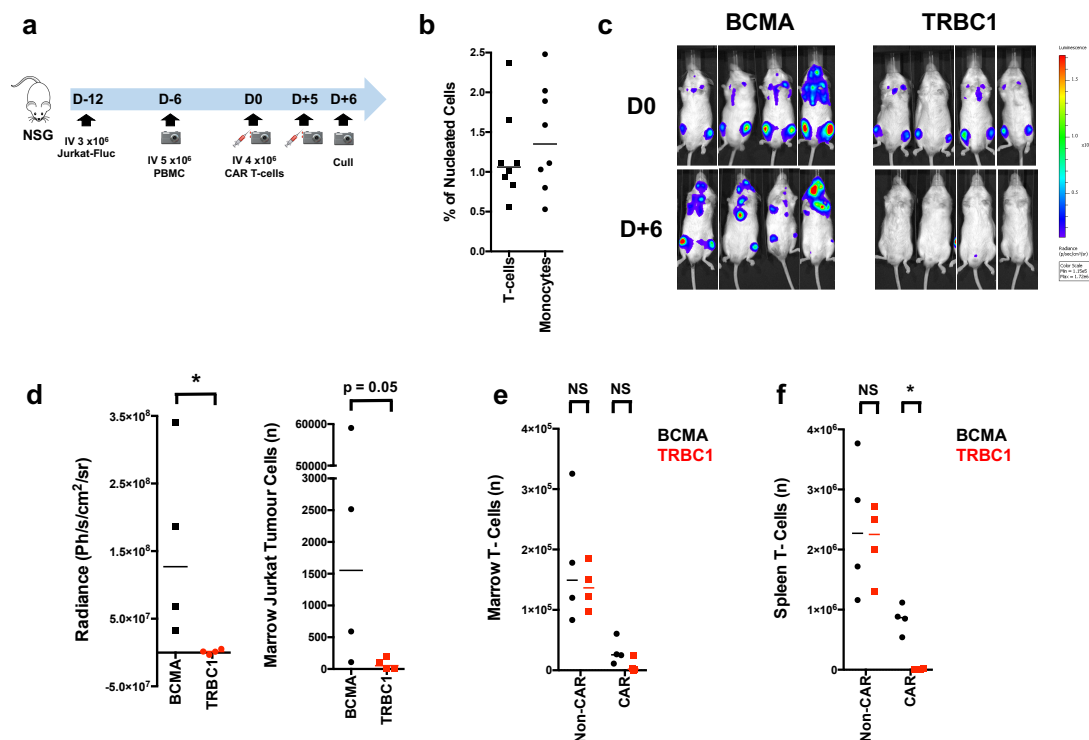
1047 **Supplementary Figure 4:** Efficacy of anti-TRBC1 CAR against TRBC1+ Jurkat
1048 tumour in human PBMC-engrafted mouse model. (a) Flow diagram of experiment (b)
1049 Engraftment of human peripheral blood cells at D6 following PBMC injection (c)
1050 Bioluminescence imaging of Jurkat tumour at D0 and D+6 following CAR injection
1051 (85% CAR+) (d) Quantification of residual Jurkat tumour by bioluminescence imaging
1052 (left) and flow cytometry of bone marrow (right). No Jurkat cells were present in spleens
1053 of either group. (e) Quantification of normal non-Jurkat T-cells in marrow. (f)
1054 Quantification of normal non-Jurkat T-cells in spleen. Anti-BCMA CAR-treated mice =
1055 black, anti-TRBC1 CAR-treated mice = red. PBMCs and effector T-cells were derived
1056 from the same healthy donor. Human monocytes were identified as CD45+CD3-CD19-
1057 CD11b+. Jurkat tumour cells were identified as CD45+CD3+CD19+CD4dim, normal
1058 T-cells were identified as CD45+CD3+CD19-RQR8-CD4+CD8- or CD45+CD3+CD19-
1059 RQR8-CD4-CD8+, and CAR T-cells were identified as CD45+CD3+CD19-RQR8+. * p
1060 < 0.05. Horizontal lines represent median values. All statistical comparisons used
1061 Mann-Whitney U-test. PBMC = peripheral blood mononuclear cells, CAR = chimeric
1062 antigen receptor, BCMA = B-cell maturation antigen. NS = non-significant

1063